

RADIOTELESCOPE LOW RATE TRACKING USING DITHER

Wodek Gawronski and Ben Parvin

Jet Propulsion Laboratory, California Institute of Technology, Pasadena, CA 91109

Abstract - Radiotelescope access to a certain part of the sky requires very low tracking rate in azimuth. At low rates, the magnitude of the dry rolling friction torques at the telescope wheels cause a non-smooth azimuth motion and the limit cycling of a telescope, which, in turn, deteriorates its pointing precision. The improvement of the low-rate tracking pointing through the dither implementation is discussed in this paper.

Dither is a high-frequency external signal injected into a system, with frequency much higher than the system dynamics. It has long been known that the injection of high-frequency signals into nonlinear electrical circuits drastically reduces the system limit cycles. We have recently identified a similar phenomenon in the limit cycling behavior of large wheel-and track radiotelescopes and microwave antennas. The high frequency signal excites local vibrations that overcome the friction-stiction torque between the wheels and the track. The vibrations, however, do not propagate through the telescope structure - thus not impacting its pointing performance. We showed through nonlinear simulations that the limit cycle amplitude of the National Radio Astronomy observatory's 100-meter radiotelescope was dramatically reduced when dither was applied, and that its pointing accuracy at low rates was significantly improved. The implementation of the dither to the radiotelescope control system is comparatively simple as it requires rather trivial modifications of the controller software and hardware. Therefore dither is a reasonable control design option for tracking improvement at low rates.

I. Introduction

Many radiotelescopes cannot precisely point at a certain part of the sky that requires tracking with very low azimuth angular rates (approximately lower than 0.4 mdeg/s). This part is about 5% of the sky. On the other hand, microwave antennas in certain tasks, such as stability measurements, are required to point at a gee-synchronous satellite. The satellite, however, is not completely stationary, it has slow movements of **0.06** mdeg/s. For such slow rates, dry rolling friction is observed at the antenna drives that cause an unwanted increase of pointing error.

In this paper we analyze the National Radio Astronomy Observatory's Green Bank **Telescope** located in West Virginia. It is one of the two worlds largest articulated radiotelescopes (its 100-meter-diameter main reflector is of the same size as the reflector of the Effelsberg radiotelescope in Germany). The Green Bank Telescope has a unique configuration characterized by the off-set reflector (see Fig. 1). The telescope's size and weight create difficulties in precision tracking. One of them is observed during tracking at low rates. It was shown in Ref.[1] that for rates lower than **0.3** mdeg/sec a non-smooth telescope motion with breakaway may occur. The peak-to-peak tracking error due to friction is 1.4 mdeg.

A high-frequency external signal injected into a system (its frequency much higher than the system dynamics) is called a dither [2,3]. It has long been known that injection of high-frequency signals into a nonlinear system results in eliminating the system limit cycles [2,3,4,5]. This phenomenon was detected in electrical circuits by Appleton in 1922. In this report we will show that the implementation of the dither will improve the telescope pointing at low tracking rates. High frequency dither signal excites local telescope

vibrations only (at the wheels), thus breaking the friction-stiction phenomena. The vibrations are not transmitted through the telescope structure - thus not impacting its pointing performance.

II. Dry Friction Model

The telescope's non-linear dynamics, at low rates, is caused by the dry friction phenomenon. Friction is a torque, or a force, that depends on the relative velocity of the moving surfaces. In the Coulomb friction model it is constant after the motion begins, and this constant is called the Coulomb friction torque. At zero speed, the friction torque is equal and opposite to the applied torque, unless the latter one is larger than the stiction torque. In this case, the friction torque is equal to the stiction torque. The stiction torque is a torque at the moment of breakaway and is larger than the Coulomb torque. A diagram of the friction torque versus relative velocity is shown in Fig.2.

Many friction models have been developed, see for example Refs.[2,6,7,8,9,10]. They reflect different aspects of the friction phenomena and their usefulness depends on application purposes. The model presented below combines basic physical properties of the dry friction with the numerical features that improve digital simulations. It is the most often utilized in the antenna industry since its accuracy for the antenna tracking purposes has been tested at many existing telescopes and antennas. In this model, denote v the telescope wheel velocity, and $v_c > 0$, a wheel velocity threshold which is a small positive number. Denote T_c the Coulomb friction torque, and T_s the stiction torque, then the friction torque model, T , is defined as follows:

$$T = \begin{cases} -T_c \operatorname{sign}(v) & \text{for } |v| > v_c, \\ -\min(|T_d|, T_s) \operatorname{sign}(T_d) & \text{for } |v| \leq v_c, \end{cases} \quad (1a)$$

where

$$\operatorname{sign}(v) = \begin{cases} 1 & \text{for } v > 0 \\ 0 & \text{for } v = 0 \\ -1 & \text{for } v < 0 \end{cases} \quad (1b)$$

and T_d denotes the total applied torque. In this model, if the surfaces in a contact develop a measurable relative velocity, such that $|v| > v_c$, the friction torque is constant, directed opposite to the relative speed. If

the relative velocity is small, namely, within the threshold, ($|v| \leq v_c$) the torque does not exceed neither the stiction torque nor the applied torque and is directed opposite to the applied torque. The velocity threshold v_c is implemented for numerical purposes: numerically the zero state does not exist, therefore the threshold represents the numerical zero.

It follows from Eq.(1a) that in order to determine the friction torque T one has to know:

- the Coulomb friction torque T_c ,
- the stiction (breakaway) torque T_s ,
- the applied torque T_d ,
- the wheel rate v ,
- the wheel rate threshold v_c .

Each variable is determined as follows.

The Coulomb friction torque is proportional to force F which is normal to the surface

$$T_c = \mu r F \quad (2)$$

where r is the wheel radius and μ is the friction coefficient. For hard steel $\mu=0.0012-0.002$.

The stiction (breakaway) torque T_s is most often assumed to be 20 to 30% higher than the Coulomb friction, that is

$$T_s = a T_c, \quad \text{where } a = 1.2 - 1.3 \quad (3)$$

The total applied torque T_d is determined from the plant dynamics as follows. Let the discrete state-space equation of the plant (which includes the telescope structure and its drives) be

$$x(i+1) = A_d x(i) + B_{dr} r(i) + B_{df} T(i), \quad (4a)$$

$$v(i+1) = C_d x(i+1) \quad (4b)$$

In this model, Δt denotes sampling time, i denotes the i th sample, $v(i)$ is the wheel rate at time instant $i \Delta t$, $x(i)$ is the plant state at the instant $i \Delta t$, $r(i)$ is the telescope angular input rate, and $T(i)$ is the friction azimuth torque. Additionally, A_d is the telescope discrete-time state matrix, B_{dr} and B_{df} are telescope rate and friction torque input matrices, and C_d is the

wheel rate output matrix. Left-multiplying Eq.(4a) by C_d gives

$$\begin{aligned} v(i+1) &= C_d x(i+1) = \\ C_d A_d x(i) + C_d B_{dr} r(i) + C_d B_{df} T(i) \end{aligned} \quad (5)$$

According to the friction model, for the wheel rate being within the threshold, i.e. such that $|v(i+1)| \leq v$, one obtains $v(i+1) = 0$, thus from Eq.(5) one obtains

$$T(i) = -\frac{C_d}{C_d B_{df}} (A_d x(i) + B_{dr} r(i)), \quad (6)$$

and the applied torque T_d is opposite to the friction torque T

$$T_d(i) = \frac{C_d}{C_d B_{df}} (A_d x(i) + B_{dr} r(i)), \quad (7)$$

The wheel rate threshold v , was assumed 0.67 mdeg/s.

III. Explaining Dither Action Using Linearized Model

There are many ways to reduce the system dynamics due to friction. Most of them are based on closed-loop compensation [2,3,1 1,12,1 3]. Here, we apply an open-loop technique by dithering the driving torque. The block diagram of the rate-loop system with the dry friction and the rate dither is shown in Fig.3. in this diagram, according to Eq.(1), the dry friction torque T is a nonlinear function of the azimuth wheel rate v and the drive torque T_d .

In order to describe the dither action we need to consider the torque at the azimuth wheel. For low rates, the driving torque T_d is smaller than the dry friction torque T_s , causing the telescope to stop. While resting, the error between the commanded position and the actual telescope position increases. In the closed-loop configuration increased error causes to increase the driving torque T_d , and eventually the movement of the telescope is observed. The cycle repeats itself and is called limit cycling. The plots of the telescope cross-elevation pointing, pinion torque, pinion angle and rate in this limit cycling are shown in Figs.4a,b and 5a,b, respectively.

A harmonic dither of amplitude d_o and period t_o

$$d(t) = d_o \sin \frac{2\pi t}{t_o} \quad (8)$$

is introduced at the telescope rate input. When dither is implemented the torque level at the wheel is raised. But the increase is not a constant one: it varies harmonically (see Fig.6a,b). If the amplitude of the driving torque T_d exceeds the friction torque, the telescope is moving continuously and the limit cycling is overcome. Due to the high dither frequency, (high, when compared to the telescope dynamics) the harmonic movement is a local phenomenon at the wheels. It is not propagated through the telescope structure, having very low impact on the structural dynamics, and consequently on the telescope pointing.

The above heuristic explanation of the dither action can be derived more formally. Consider the continuous-time telescope model with the nonlinear friction torque $T(v)$, driven by the command rate, r , and dither, d

$$\begin{aligned} \dot{x} &= Ax + B_r(r+d) + B_f T(v), \\ v &= Cx \end{aligned} \quad (9)$$

The parameters (A, B_r, B_f, C) are the of the continuous-time counterparts of the discrete-time parameters $(A_d, B_{dr}, B_{df}, C_d)$ as in Eq.(4), and $x(t)$ is the continuous-time state variable of the plant. This equation is averaged over the dither period t_o . The average value x_a of x is defined as

$$x_a(t) = \frac{1}{t_o} \int_t^{t+t_o} x(\tau) d\tau. \quad (10)$$

Next, note that in Eq.(9) the average value of the rate command is almost the same as the instantaneous value, since the command changes insignificantly over the period t_o , i.e., $r(t) \cong r(t+t_o)$. The average value $\hat{T}(v)$ of the nonlinear torque $T(v)$ is obtained from the dry friction torque as in Eq.(1). The velocity threshold v , in this equation is assumed zero (the non-zero threshold was previously introduced to avoid numerical difficulties in simulations). Thus, the wheel friction torque is given as

$$T = -T_c \text{sign}(v + d) \quad (11)$$

The average torque \hat{T} is called the smooth image of the dry friction torque. The smooth image \hat{T} is defined as $\hat{T} = \frac{1}{T_c} \int_{t_o}^{t_o+T_c} T d\tau$, therefore one obtains

$$\hat{T}(v) = \frac{1}{T_c} \int_{t_o}^{t_o+T_c} T(v) d\tau = -\frac{1}{T_c} \int_{t_o}^{t_o+T_c} T_c \text{sign}(v+d) d\tau = -\frac{2T_c}{\pi} \arcsin\left(\frac{v}{d_o}\right) \quad (12)$$

The plot of \hat{T} with respect to $\frac{v}{d_o}$ for $T_c = 1$ is shown in Fig.7. One can see from this figure that although the dry friction T is a discontinuous function of the rate, its smooth image \hat{T} is, by definition, a smooth function of the rate. It also follows from Fig.7 that the smooth image exists only for the dither amplitudes that extend the wheel rate, i.e., for $d_o > v$. This is quite understandable since for the dither amplitude smaller than the wheel rate there is no change in the friction torque (see Eq.(11)).

Since the function \hat{T} is smooth it can be linearized for small rate variations. That is, for small wheel rate v that is proportional to the rate of the command r , $v = k_r r$, one obtains

$$\left. \frac{d\hat{T}}{dv} \right|_{v=0} = -\frac{2T_c}{\pi d_o} \quad (13)$$

or

$$\hat{T}(d_o) \cong k_o r, \quad k_o = -\frac{2T_c k_r}{\pi d_o} \quad (14)$$

The plot of linearized \hat{T} in Fig.7, shown as a dashed line, reveals a good coincidence with \hat{T} for $v < 0.5d_o$.

Introducing Eq.(14) to the averaged Eq.(9) one obtains the following linear system

$$\dot{x}_a = Ax_a + B_{r_o} r + B_r d, \quad y_a = Cx_a \quad (15a)$$

with the input matrix B_{r_o} in the form

$$B_{r_o} = B_r + k_o B_n \quad (15b)$$

The above equation proves that the system dynamics with dry friction and dither is linear one. Also, notice that the dither input has no significant impact at the telescope pointing. Let us write the pointing y_a as a superposition of the pointing (-VW) due to the input r and the pointing (y_{ad}) due to the dither input d , i.e., $y_a = y_{ar} + y_{ad}$. Notice that the dither is of high frequency, therefore the response y_{ad} is negligible when compared to y_{ar} , thus $y_a \cong y_{ar}$. The latter shows, that the dither action makes the telescope dynamics linear, but it does not show itself at the output, thus the telescope pointing performance is not affected.

IV. Nonlinear Simulation Results

Typically, the dither signal should be injected just ahead of the nonlinearity. In the case of the Green Bank Telescope it is a rate command at the telescope azimuth drives. In this case the dither is simply added to the feed-forward command generated by the controller computer.

The dither amplitude and frequency are determined as follows. The frequency must be much higher than the telescope dynamics. Since no significant telescope dynamics is observed above 10 Hz, the dither frequency 30 Hz ($\omega_o = 188.5rd/s$) is chosen. The dither amplitude depends on the level of friction torque. Dry friction torque for tracking at a rate of 0.3 mdeg/s is shown in Fig.4b and is smaller than 5642 N-m (50,000 lb-in). For this friction level the dither amplitude was determined to be 0.18 deg/s. The selection process included the telescope pointing simulations with various dither amplitudes. The plot of dither amplitude versus cross-elevation pointing is shown in Fig.8. It follows from this figure that the cross-elevation error is the smallest for an amplitude of 0.18 deg/s. The plot of the cross-elevation pointing and the pinion angle for the above dither amplitude are shown in Fig.9a,b. The plots show the smooth pinion angle profile and small pointing error. Additionally, Fig. 10 shows the elevation and cross-elevation errors for the telescope with and without the dither for a time segment of [35, 40] s, when the telescope motion is already stationary. The maximum elevation error dropped 14 fold, from 0.19 to 0.014 mdeg, and the maximum cross-elevation error dropped 18 fold, from 1.4 to 0.08 rndeg.

Acknowledgment

The authors would like to thank Robert Hall and Lee King of the National Radio Astronomy Observatory, Charlottesville, VA, for their valuable discussions.

References

- [1] W. Gawronski, and B. Parvin, "Analysis and Design of the GBT Control System," NRAO *Internal Document*, September, 1995.
- [2] B. Armstrong-Helouvry, P. Dupont, and C. Canudas de Wit, "A Survey of Models, Analysis Tools and Compensation Methods for the Control of Machines with Friction," *Automatic*, vol.30, No.7, 1994, pp.1083-1138.
- [3] P.E. Dupont, and E.P. Dunlap, "Friction Modeling and PD Compensation at Very Low Velocities," *Journal of Dynamic System, Measurement, and Control*, vol. 117, No. 1, 1995, pp.8-14.
- [4] S. Lee and S.M. Meerkov, "Generalized Dither," *International Journal of Control*, vol.53, No.3, 1983, pp.741-747.
- [5] S. Mossaheb, "Application of a Method of Averaging to the Study of Dithers in Non-linear systems," *International Journal of Control*, vol.38, No.3, 1983, pp.557-576.
- [6] B. Armstrong-Helouvry, P. Dupont, and C. Canudas de Wit, "Friction in Servo Machines: Analysis and Control Methods," *Applied Mechanics Review*, vol.47, No.7, 1994, pp.275-305.
- [7] P.-A.J. Bliman, "Mathematical Study of the Dahl's Friction Model," *European Journal of Mechanics, A/Solids*, VOL. 11, No.6, 1992, pp.835-848.
- [8] C. Canudas de Wit, H. Olsson, K.J. Astrom, and P. Lischinsky, "A New Model for Control of Systems with Friction," *IEEE Trans. on Automatic Control*, vol.40, No.3, 1995, pp.419-425.
- [9] P.R. Dahl, "Solid Friction Damping of Mechanical Vibrations," *AIAA Journal*, vol. 14, No.12, 1976, pp.1675-1682.
- [10] S. Dimova, "Comparison and Experimental Verification of Two Techniques for Friction Force Representation," *Computers & Structures*, vol.60, No.1, 1996, pp.11-19.
- [11] L. Cai, and G. Song, "Joint Stick-Slip Friction Compensation of Robot Manipulators by Using Smooth Robust Controllers," *Journal of Robotic Systems*, vol. 11, No.6, 1994, pp.451-469.
- [12] P.E. Dupont, "Avoiding Stick-Slip Through PD Control," *IEEE Trans. on Automatic Control*, vol.39, No.5, 1994, pp.1094-1097.
- [13] S.C. Southward, C.J. Radcliffe, and C.R. MacCluer, "Robust Nonlinear Stick-Slip Friction Compensation," *Journal of Dynamic Systems, Measurement, and Control*, vol. 113, 1991, pp.639-645.

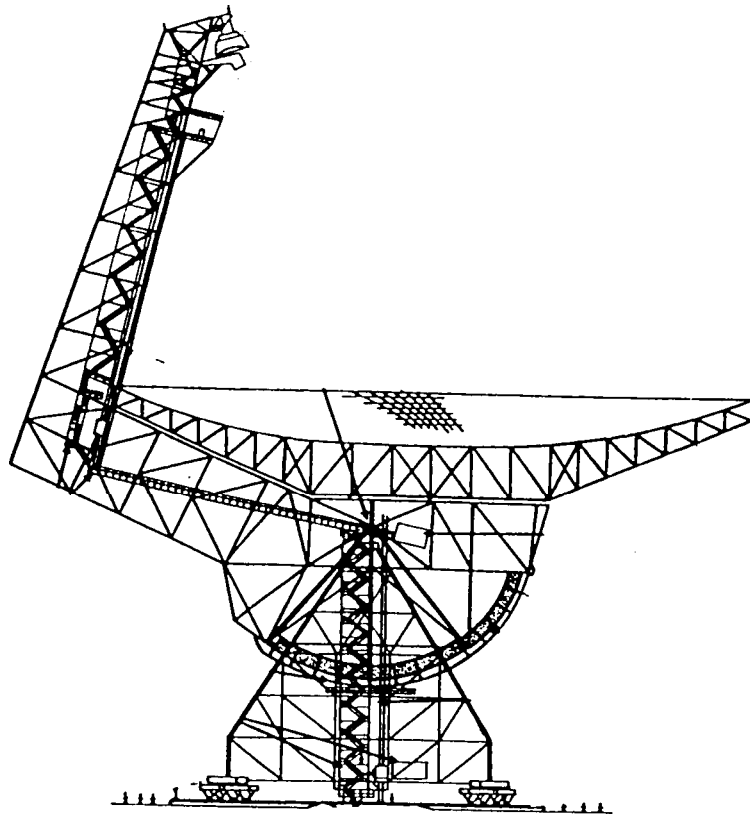


Figure 1. National Radio Astronomy Observatory Green Bank radiotelescope

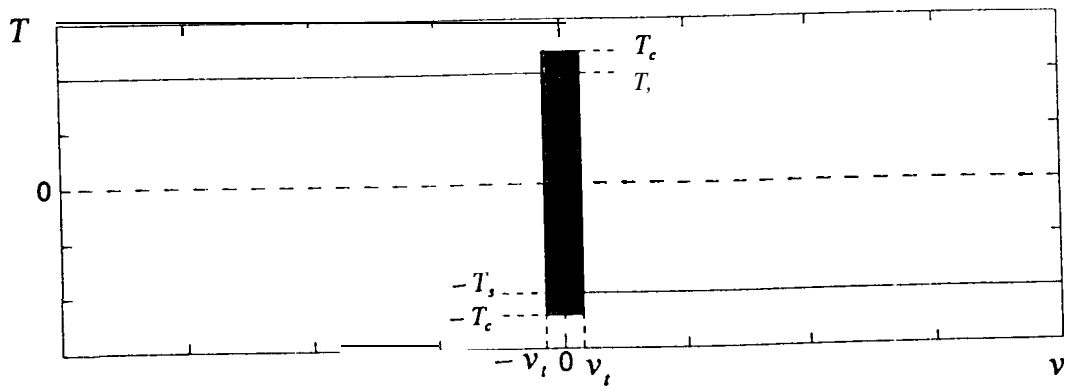


Figure 2. Friction torque versus rate.

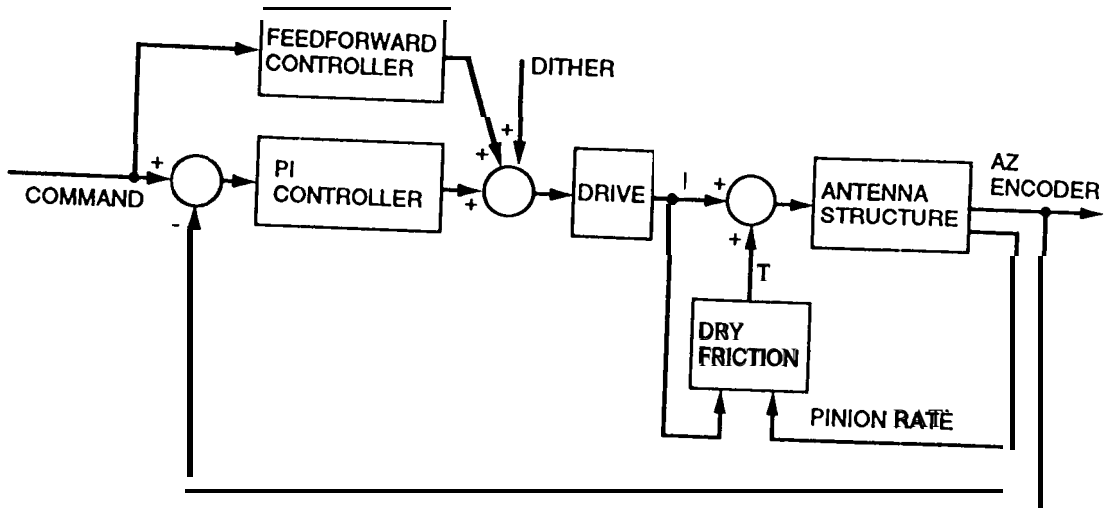


Figure 3. Azimuth control system with dry friction and dither.

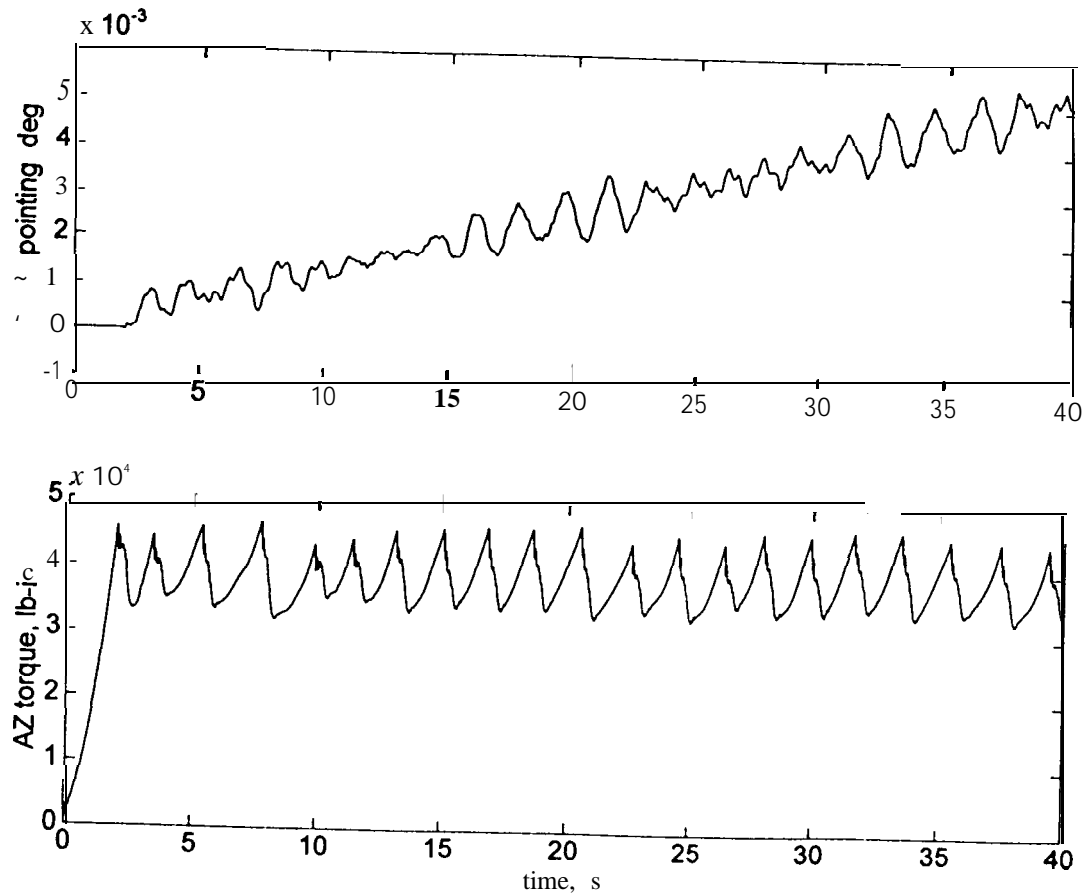


Figure 4. Simulated tracking with friction at rate 0.3 mdeg/s: a) cross-elevation pointing, b) azimuth pinion torque.

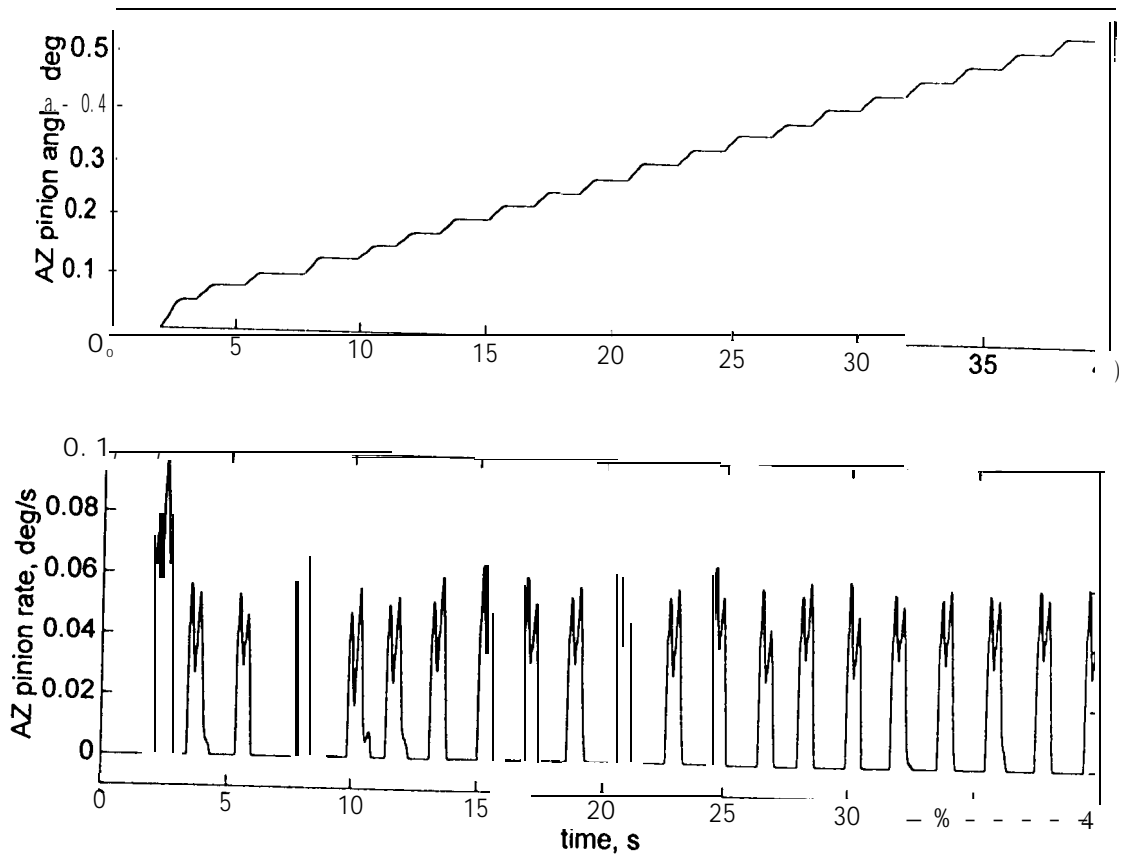


Figure 5. Simulated tracking with friction at rate 0.3 mdeg/s: a) azimuth pinion angle, b) azimuth pinion rate.

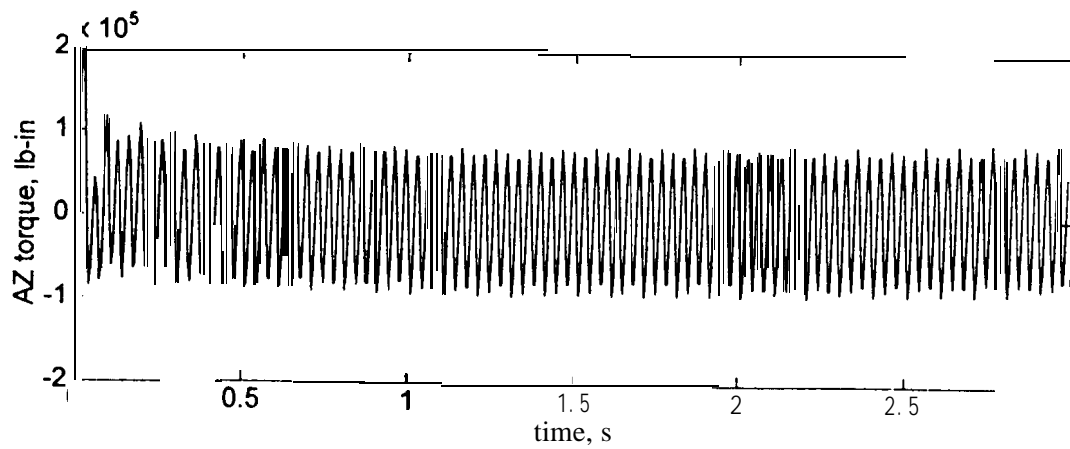


Figure 6. Azimuth pinion torque with dither.

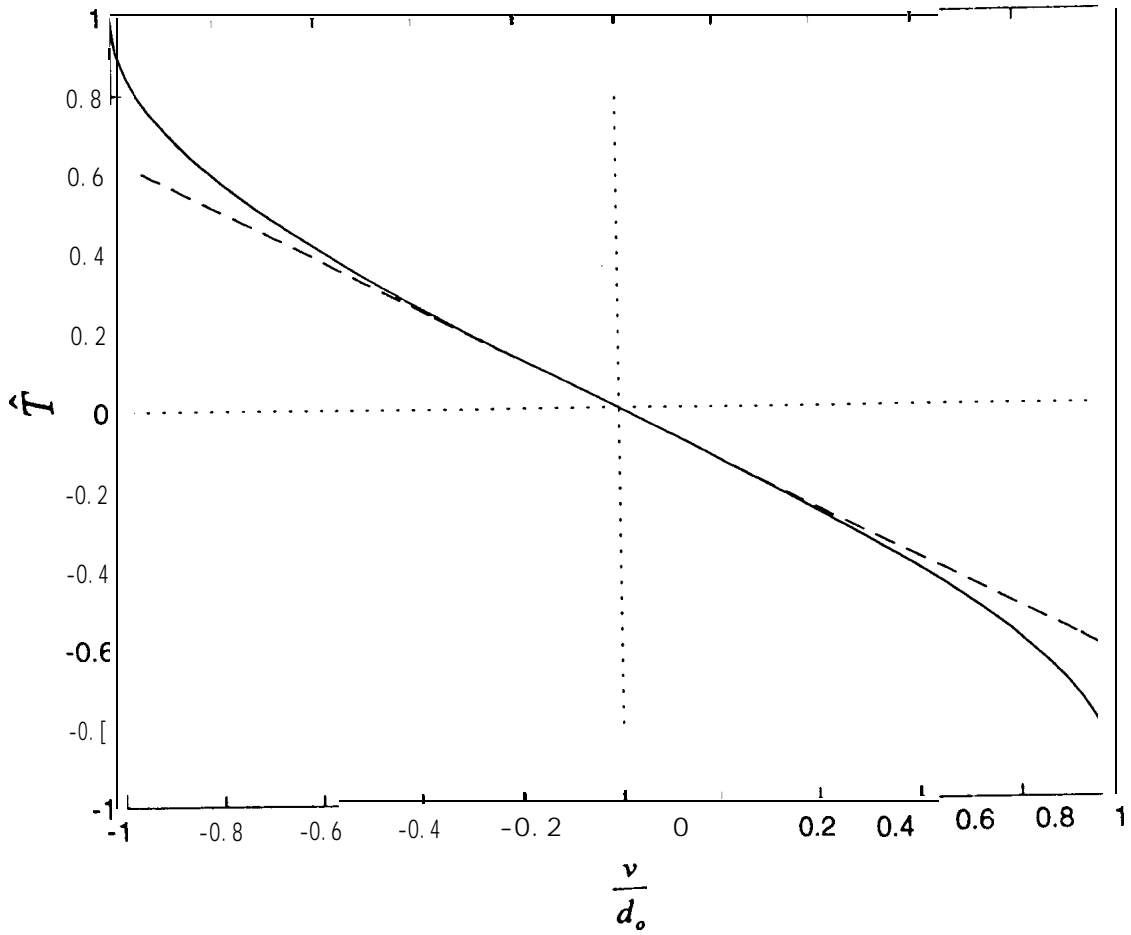


Figure 7. Smooth image of dry friction (—) and the linearized image (---).

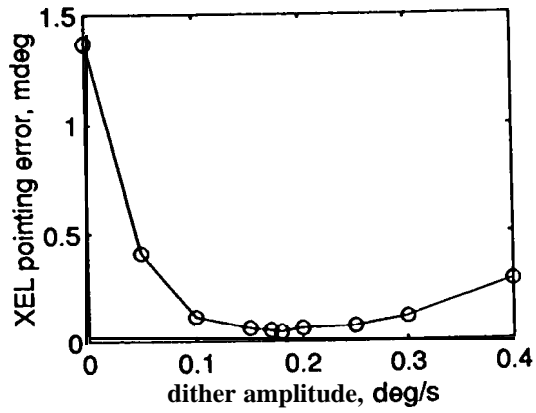


Figure 8. Cross-elevation pointing vs. dither amplitude.

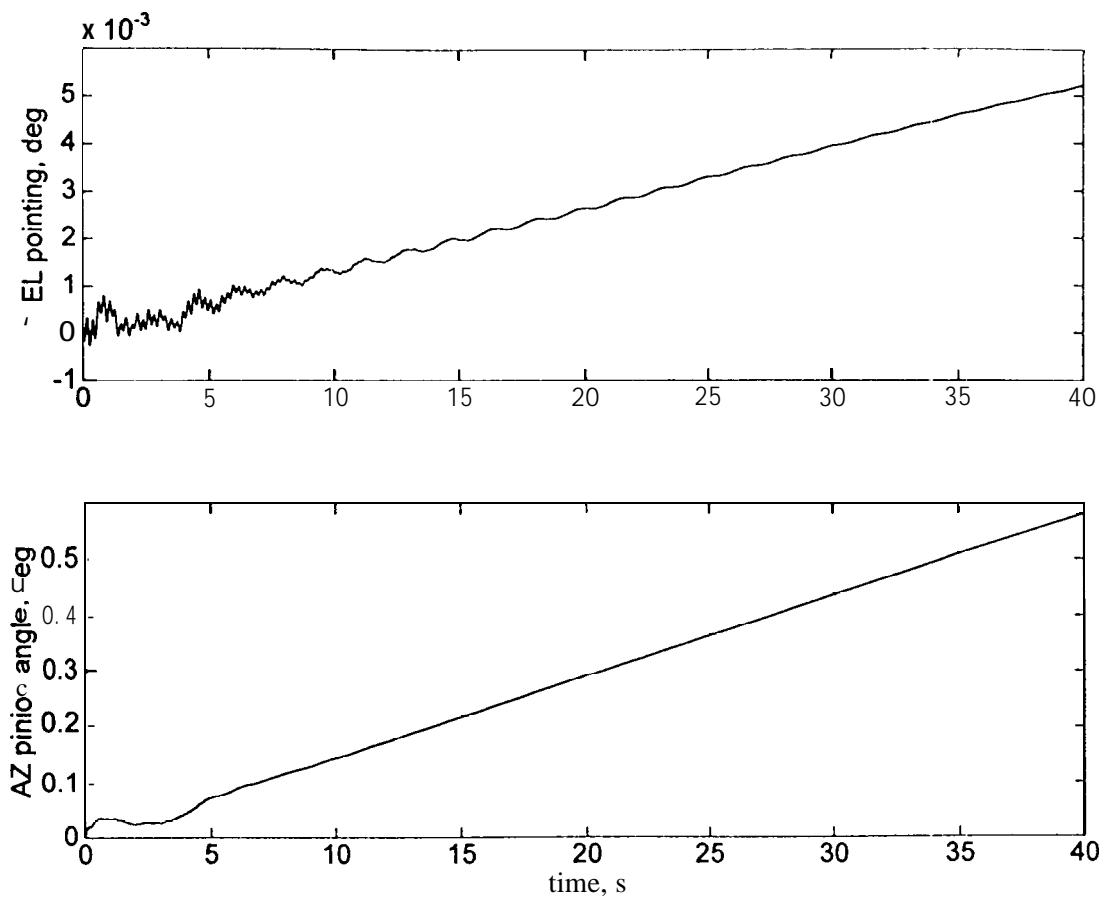


Figure 9. Tracking at 0.3 mdeg/s with dry friction, and dither 0.18 deg/s: a) cross-elevation pointing error, b) azimuth pinion angle.

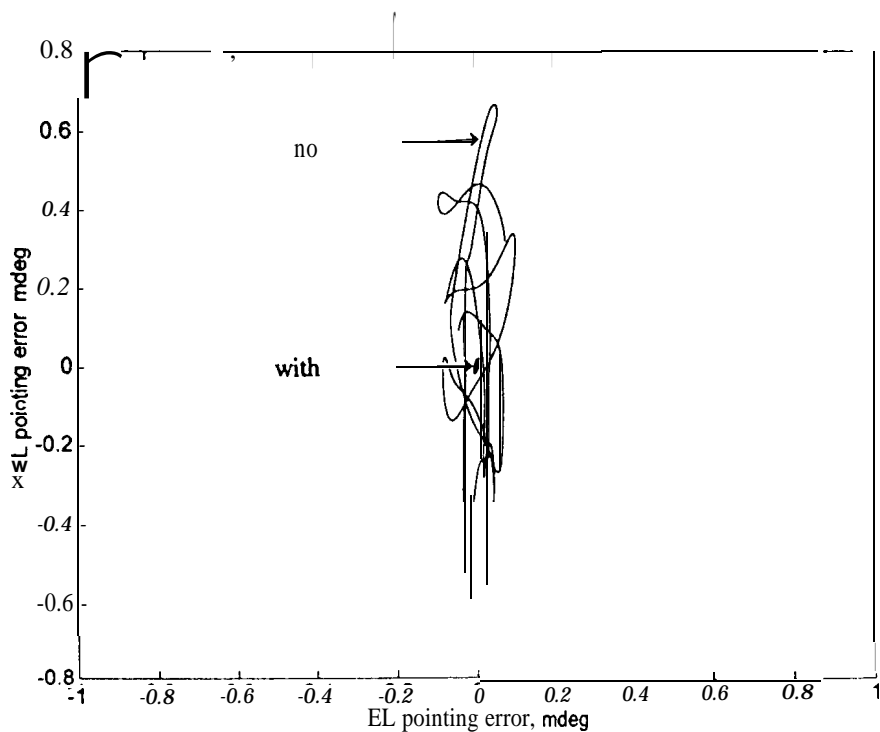


Figure 10. Elevation and cross-elevation errors for time segment [35, 40] s, without and with dither.